Z. Phys. A - Atoms and Nuclei 304, 41-48 (1982)

Zeitschrift für Physik A Atoms and Nuclei

Analysis of Autoionization Resonances in the Hg $6s^2$-Photoionization by Measurements of Photoelectron Polarization

F. Schäfers, G. Schönhense, and U. Heinzmann

Fritz-Haber-Institut der Max-Planck-Gesellschaft, Berlin, Germany,
Physikalisches Institut der Universität Münster, Synchrotron der Universität Bonn, Federal Republic of Germany

Received September 7, 1981; revised version October 5, 1981

Measurements of the spin polarization of photoelectrons in the autoionization region of the Hg $6s^2$-subshell using circularly polarized synchrotron radiation and using unpolarized light from rare gas discharge lamps are reported. The results obtained show a pronounced structure across the resonances. Together with data of the cross section and its angular distribution these data from a complete parameter set for the determination of the transition matrix elements and the phase difference of the continuum wavefunctions. Evidences for strong configuration interaction and channel mixing between the open and closed channels were found. The matrix elements and their ratio vary strongly across the resonances and the relative phase shows some changes of sign. A change of the relative phase by π across an autoionization resonance, predicted by Fano, has been verified experimentally for the triplet resonance.

1. Introduction

Spin polarization of photoelectrons has been proved experimentally to be a common rule rather than an exception for most atomic and molecular systems [1, 2]. One has to distinguish between two different kinds of "production" of spin polarization of photoelectrons from unpolarized targets:

The first kind theoretically predicted by Fano in 1969 [3], and shortly thereafter experimentally found at Cs [4], is a spin-polarization transfer from the ionizing light to the photoelectrons produced (Fano effect). For this kind of experiment, therefore, circularly polarized light is needed, whose spin is directed either into the direction of propagation of the light (σ^+ light) or away from it (σ^- light). In the experiment one has in general elliptically polarized radiation. Photon and photoelectron spin-polarizations are proportional to each other, so that a spin-polarization transfer can be defined to be the ratio of the spin polarization of the photoelectrons to the circular polarization of the ionizing radiation. This spin transfer is generally different from zero for photoionization of atoms and molecules even if the photoelectrons produced are extracted by an electric field regardless of their directions of emission. In this case the spin polarization transfer defined above is a "total spin transfer" A, analogous to studies of the "total photoionization cross section", where all electrons or ions produced are also collected by an electric field. This spin parameter A can also be seen to be an average photoelectron polarization itself, but only under the (theoretical) assumption that the ionizing radiation is completely circularly polarized. The "spin-transfer mechanism" is the spin-orbit interaction [5]; without spin-orbit interaction no photoelectron polarization can occur.

In subshells with $l>0$ spin-orbit interaction produces an energetical fine-structure splitting of the atomic ground and/or ionic final states resulting in different binding energies of the valence electrons for different total angular momenta of the atoms or the ions. Furthermore, spin-orbit interaction affects the continuum states in such a way that the wave functions describing the photoelectrons - and with it the transition matrix elements - depend on the orientation of the spin with respect to the orbital angular momentum of the photoelectron, i.e. on $j=l\pm 1/2$. The latter effect is commonly called relativistic, but it can be treated in non-relativistic theories in an "ad hoc"-fashion, too [6].

The second kind is a spin polarization which can be

0340-2193/82/0304/0041/$01.60

found even if unpolarized or linearly polarized light is used [7–9] and whose experimental observation also presumes the existence and/or the resolution of the spin-orbit interaction. This polarization and its angular dependence [10] is determined by the parameter ξ and is based upon an interference effect between the wavefunctions of different continuum states.

Studies of spin polarization phenomena are performed in order to get detailed information about the photoionization process and to understand the influences of the many-electron system – such as correlations i.e. configuration interaction [11, 12] – on the photoelectrons. Especially the combination of the polarization results with other data, such as the photoionization cross section σ and the asymmetry parameter β (describing the angular dependence of the differential cross section), allows the complete determination of the dipole matrix elements and of the phase differences between the continuum wave functions. Due to the dipole selection rules ($\Delta l = \pm 1$, $\Delta j = 0, \pm 1$) the number of the quantum mechanical quantities to be determined is limited to five.

It is the purpose of this paper to present measurements of the total spin transfer A as well as of the spin parameter ξ for photoionization of the $6s^2$-subshell of Hg atoms. For comparison with the data of Hg a few experimental results at Cd with respect to the corresponding $5s^2$-subshell are also presented.

Starting from the threshold the ionization continuum is masked by autoionization processes due to excitation of a d-electron. For s-electrons there is no fine-structure splitting in the bound states, and consequently non-relativistic theories predict $A = \xi = 0$ and $\beta = 2$ [13]. Therefore all polarization effects arise from spin-orbit interaction in the continuum states.

Recent measurements of the β-parameter in the autoionization region of Hg [14–16] yielded strong deviations from the Cooper-Zare value $\beta = 2$ across the resonances, indicating the strong influence of the spin-orbit interaction on the continuum states in the region of resonances. As the photoionization of s-subshells is described by only two matrix elements (transitions into $\varepsilon p_{1/2}$ and $\varepsilon p_{3/2}$ continua) and by one phase shift difference between the $\varepsilon p_{1/2}$ and $\varepsilon p_{3/2}$ continuum wave functions, experimental data of A, ξ and β together with cross section results form a complete parameter set for the determination of these three quantities. This is also reported in detail in this paper.

Polarization phenomena in autoionization resonances have been the subject of some theoretical work, especially on rare gases using the multichannel quantum defect theory [9, 17]. Cherepkov [18] used polarization data for the identification of resonances. Kabachnik and Sazhina [19] gave a general expression for the shape of the polarization across a resonance, whose applications are limited, however, by the treatment of isolated resonances only. Up to now no calculations of the Hg $6s^2$ autoionization region are available.

The measurements of the spin parameter A were done with synchrotron radiation [20], which combines the advantage of a tuneable light source – which allows the detailed observation of resonance phenomena – with a high degree of circular polarization. (In fact, a synchrotron or electron storage ring is the only source of circularly polarized radiation in the VUV wavelength range above 10 eV photon energy.)

Already implicitly included in Schwinger's theory [21] Sokolov and Ternov [22] and Westfold [23] explicitly showed that synchrotron radiation consists of two linearly polarized components oscillating perpendicular to each other with a fixed phase relation. The component polarized perpendicular to the plane of the orbiting electrons is emitted only in off-axis directions [24, 25]. The radiation emitted into the synchrotron plane, therefore, is completely linearly polarized. Since the two components have a phase difference of 90 degrees relative to each other, outside the plane the radiation is elliptically polarized with a high degree of circular polarization.

The experimental arrangement at the 2.5 GeV synchrotron in Bonn will be briefly presented in section 2. First experimental results obtained with the rare gases Ar, Kr, Xe using this apparatus together with other experimental data allowed a complete determination of the matrix elements as well as of the phase-shift differences between the continuum wave functions [26–28].

The measurements of the spin parameter ξ were performed using unpolarized radiation from rare gas discharge lamps in a photoionization experiment, where the photoelectron emission is resolved as to the energy, the emission angle and the spin. Its experimental setup is described in this volume as well [29].

2. Experimental Setup

The experimental arrangement for the measurement of the spin-polarization parameter A is shown in Fig. 1. The radiation emitted tangentially from the electron beam in the synchrotron is monochromated by a 10 m normal-incidence monochromator consisting of a plane holographic grating (4960 lines/mm)

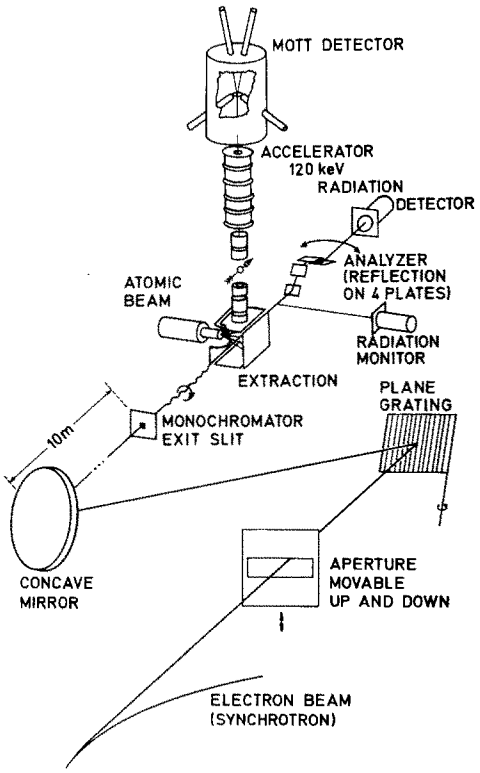

Fig. 1. Experimental set-up for the measurement of the spin polarization parameter A

and a concave mirror, by which the radiation is focussed onto the exit slit in a 1:1 image. As the circular polarization of the radiation is the crucial point of the experiment, only normal incidence reflections at the grating (Littrow mounting) and the mirror surface could be used in order to minimize depolarization of the Stokes parameter describing the circular polarization; furthermore, in contrast to other mountings of getting best linear polarization [20], the plane of dispersion is in the plane of the electron beam in order to favor s-reflection. For intensity reasons no entrance slit was used and the acceptance is limited only by the dimensions of the beam-line (21 mrad horizontal, ± 3.5 mrad vertical). The degree and the helicity of the polarization can easily be chosen by an aperture moveable in vertical direction, which transmits either the radiation emitted into the upper half (σ^- light) or into the lower half (σ^+ light) with respect to the synchrotron plane.

The circular polarization of the monochromated radiation (bandwidth 0.05 nm) is analyzed with a rotatable four-mirror arrangement (reflection at 60°, analyzing power $>99\%$). The light transmitted through the analyzer is detected by an open multiplier; a second multiplier is used to record instabilities of the light intensity.

In the VUV region from 40 nm to 100 nm the circular polarization is nearly independent of the wavelength. For the photoionization measurements the radiation emitted into a vertical angle $\psi > 1$ mrad was used yielding a circular polarization of 80% with a photon flux of some 10^9 photons $\cdot s^{-1} \cdot (0.05\ \text{nm})^{-1}$ measured with a double ionization chamber of the Samson type. A detailed description of the measurements of the circular polarization and of the absolute intensity will be given elsewhere [30].

Behind the exit slit the light hits the metal vapor, evaporated in a resistively heated furnace, formed by a capillary array and pumped by a liquid nitrogen cool trap. The photoelectrons produced are extracted by an electric field regardless of their direction of emission. After focusing and acceleration of the electrons to 120 keV the spin polarization is analyzed in a Mott detector by measuring the left-right asymmetry of the electrons scattered into 120° by a gold foil (180 $\mu g cm^{-2}$). Photoelectron intensities are normalized to constant light intensity, which was monitored by recording the electron current in the synchrotron. All measurements were performed at a synchrotron energy of 0.8 GeV. To eliminate apparatus-related asymmetries in the Mott detector three measurements (using σ^- light, σ^+ light and no light to determine the background count rate) were performed. The polarization was determined according to [31] taking into account the forward counters placed at a scattering angle of 13° in order to control the apparatus-related asymmetries, too. All polarization values measured are normalized to 100% circular polarization of the light, i.e. the "total spin transfer" A (ratio of electron and photon spin polarization) is shown in the figures.

3. Results

The influence of relativistic spin-orbit interaction effects on the photoionization of s-subshells has been investigated in some theoretical [3, 32–35] and experimental [4, 28, 36, 37] work. The main interest was focused on targets and wavelength regions where the cross section shows Cooper minima; there the matrix elements for the electronic transitions $s \rightarrow \varepsilon p_{1/2}$ and $s \rightarrow \varepsilon p_{3/2}$ change their sign at slightly different energies leading to strong variations in the β parameter and to a high degree of electron polarization. This latter effect has been called the Fano effect [3].

When the direct continuum is overlapped by autoionization processes resonance behavior of the polarization similar to that of the cross section should

be expected, especially as the relative phase changes by π across the resonance [38, 39]. Measurements of the β parameter in the window resonances of Ar and Xe [40] and in the autoionization region of Hg [14–16] yielded a pronounced resonance structure.

Therefore Hg and Cd atoms with the configuration $(n-1)d^{10}\,ns^2$ ($n=5$ for Cd, $n=6$ for Hg) seemed to be a suitable and promising system for the investigation of polarization phenomena on electrons of closed s-subshells. Starting from the threshold the cross section is dominated by pronounced autoionization resonances due to excitation of d-electrons into discrete states beyond the photoionization threshold which are energetically degenerate with respect to the continuum states.

The photoionization of Hg (Cd analogously) is described by the following equation:

$$\begin{aligned} &\mathrm{Hg}(5d^{10}\,6s^2)^1S_0 + h\nu \\ &\rightarrow \mathrm{Hg}^*[(5d^9\,6s^2)\,{}^2D_{3/2}\,np_{1/2};p_{3/2};f_{5/2}]_{J=1} \\ &\qquad\quad \text{or}\quad {}^2D_{5/2}\,np_{3/2};f_{5/2};f_{7/2}]_{J=1} \\ &\rightarrow [\mathrm{Hg}^+(5d^{10}\,6s)\,{}^2S_{1/2} + e^-(\varepsilon p_{1/2};\varepsilon p_{3/2})]_{J=1} \end{aligned}$$

The last line describes the direct ionization process while the first two lines represent the autoionization process. The highly excited autoionization states are members of six different Rydberg series, three np- and three nf-series, converging to the fine-structure split d-threshold with a ${}^2D_{5/2}$ or a ${}^2D_{3/2}$ final ionic state [41].

3.1. Mercury

Figure 2 shows the experimental results of the spin parameter A in the autoionization region of Hg. In the upper part of Fig. 2 the cross section measured by Brehm [42] (curve) is shown for comparison; the points indicate the photoelectron intensities measured and fitted to the curve in the first maximum. Although the LS assignments of the resonances shown in Fig. 2 agree with those commonly used [44, 45], the autoionizing states are better described [46, 47] in the jj-coupling scheme (dissociation channels) which is also verified by the results of the present paper to be a reasonable good approximation; i.e. the photoelectron is a $p_{1/2}$-electron in the first resonance with a probability of 87‰, whereas the $p_{3/2}$-character dominates in the two other resonances (94% and 100‰, respectively). The spin-polarization parameter A of the photoelectrons ("total spin transfer") is shown in the lower part of Fig. 2: The error bars include the single statistical error as well as the uncertainty of the measurement of the

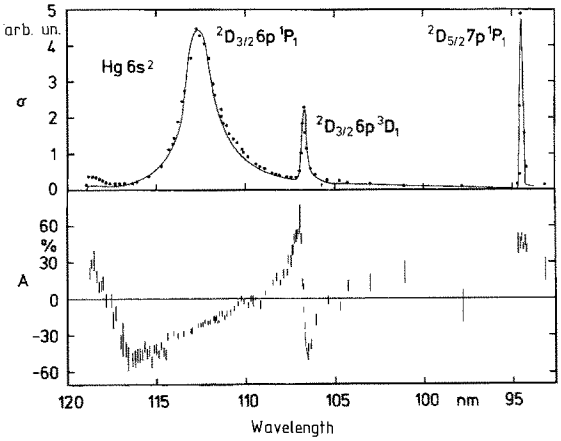

Fig. 2. Photoionization of mercury in the autoionization region upper part: cross section σ in arb. units [42] (curve), photoelectron intensity (points, this work), fitted to the curve in the first maximum, where the absolute cross section is 200 Mb [43]. Lower part: spin polarization parameter A (total spin transfer)

light polarization and of the Sherman function of the Mott detector (-0.26 ± 0.01) [31]. The bandwidth of the VUV-radiation (0.05 nm) determines the horizontal error bars, in Fig. 2 smaller than the width of the vertical error bars drawn. For intensity reasons no results could be obtained in the vicinity of the third resonance, as the cross section in the minimum of this resonance is three orders of magnitude smaller than in the maximum.

In the three resonances belonging to different series the shape of the polarization curve is quite different: It is negative in the first resonance with a change of sign left from the maximum*, in the third resonance it is positive as far as experimental results are available, while in the second resonance the polarization suddenly changes its sign from high positive to high negative values in a wavelength region less than 0.5 nm.

The structures of the electron polarization curve reflect the different configurations of the autoionizing states. In the outer singulet resonances the different orientation of the spin with respect to the orbital angular momentum of the photoelectron ($p_{1/2}$ and $p_{3/2}$, resp.) results in a negative and positive polarization, resp. Analogously, due to the $p_{3/2}$-character of the autoionizing state, one would expect a positive polarization in the second resonance. Its sign, however, changes in the resonance due to spin-flip processes, responsible in the close coupling scheme

* This change of sign may be due to the cross section minimum of the resonance which was observed at the same position in the photoelectron intensity. According to the Fano parametrization of this resonance performed by Brehm [42], however, this minimum should be located in the discrete part of the spectrum at 124.8 nm

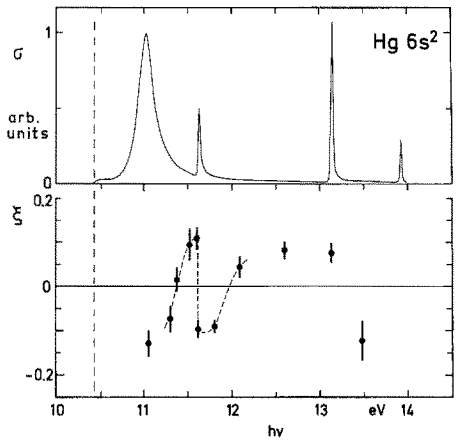

Fig. 3. Photoionization of mercury in the autoionization region upper part: cross section σ [42] (the same as in Fig. 2). Lower part: spin parameter ξ, the curve is a tentative curve drawn through the experimental results to show the resonance structure

for the high triplet character of this state. Indications for a different behavior of this resonance have already been given by measurements of the β parameter [14–16] which has a negative minimum in the resonance. In the case of s-electrons deviations from $\beta=2$ are a direct measure of the triplet character of the continuum wave-functions [48].

Figure 3 shows the experimental results of the spin parameter ξ. Opposite to the usual way used for the determination of the parameter A, here the resonances were resolved by means of photoelectron spectroscopy using an electron spectrometer and employing the undispersed many-line spectrum of H_2 and ArI lines (at $h\nu=11.63$ eV and 11.83 eV) produced in gas discharge lamps. A detailed description of the technique applied is given elsewhere [28]. The upper part of Fig. 3 shows the cross section by Brehm [42] plotted as function of the photon energy. The spin parameter ξ (lower part) varies strongly across the resonances. Similar to the A parameter (Fig. 2) the sign of ξ is different in the singulet resonances (1. and 3.) and the sign of ξ changes in the triplet resonance within an energy-interval less than 200 meV, illustrated by the tentative curve drawn through the experimental results.

In order to compare the different experimental results obtained in the autoionization region of Hg, all experimental data available are shown in Fig. 4, in the vicinity of the triplet resonance in an expanded scale:

1. total cross section σ [42, 43]
2. asymmetry parameter β [14–16]
3. spin parameter A (this work)
4. spin parameter ξ (this work).

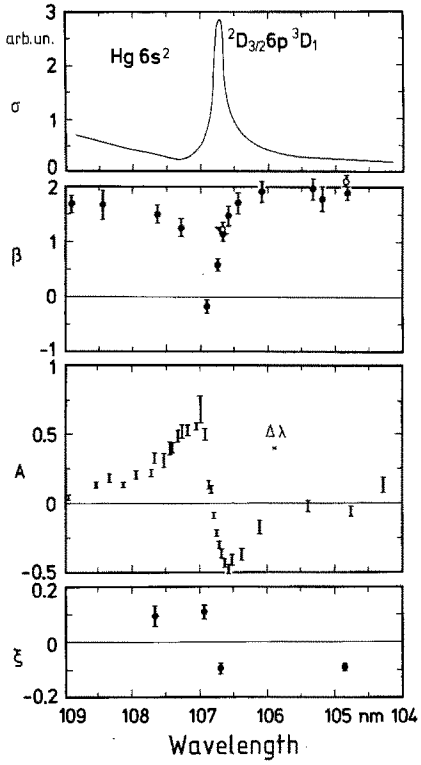

Fig. 4. Photoionization of mercury in the autoionization region cross section σ: [42, 43]. Asymmetry parameter β: [15, 16] (closed circles); [14] (open circles). Spin polarization parameter A: this work, $\Delta\lambda(=0.05$ nm) is the bandwidth of the light. Spin parameter ξ: this work

All four parameters show resonance structure:

1. The asymmetric Fano-type profile of σ is described by the parameters [42]:

$$q=6, \quad \Gamma=0.022\,\text{eV}, \quad E_0=11.607\,\text{eV}$$

2. The β parameter has a negative minimum and reaches the non-relativistic value $\beta=2$ at the high-energy side.

3, 4. The polarization parameters A and ξ change their sign in the resonance.

The advantage of a tuneable light source for the observation of resonance phenomena is clearly seen in Fig. 4. Within the experimental uncertainties for β and ξ given by the scan of the H_2 many-line spectrum and the ArI lines, the wavelength region, in which the change of sign in the polarization parameters A and ξ occurs, coincides with the resonance pattern in β, of which the experimental minimum of -0.2 may be seen to be only the upper limit. The position of the sign change of ξ and A coincides with the resonance energy E_0 determined from the parametrization of the cross section.

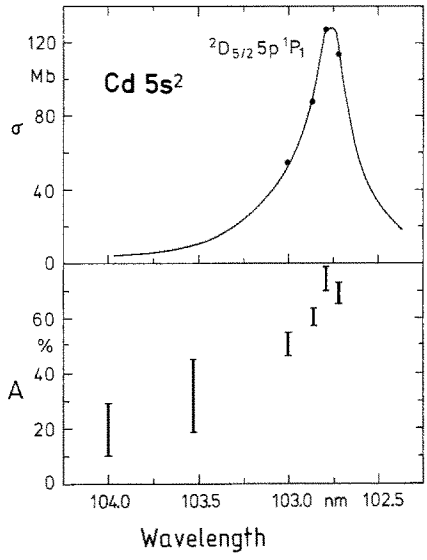

Fig. 5. Photoionization of Cd in the autoionization region. Upper part: cross section σ [49]. Photoelectron intensity (points, this work) fitted to the curve in the maximum. Lower part: spin polarization parameter A

3.2. Cadmium

Because Cd has the same electronic configuration as Hg, the experimental data of the parameter A obtained in the autoionization region (Fig. 5) thus may be compared with the data from Hg. The cross section (top) was measured by Marr and Austin [49]. The first resonance shown has the same assignment as the 3. resonance of Hg. But for the study of this type of resonance Cd has the main advantage compared with Hg, that the resonance shows a broader and more pronounced profile. Thus the spin-transfer experiment has been performed in Cd there, in addition to the Hg measurements. Analogously to Hg the spin parameter A is positive, up to 75%, and shows smooth resonance behavior as far as results are present. No experimental results for β and ξ are available in the resonance region of Cd; the data for the analysis of the photoionization process are thus far from being complete.

The high degree of polarization measured in the resonance indicates that in the region of autoionization the spin-orbit interaction in the continuum states is strongly influenced and enlarged by the coupling strength between the discrete and continuum states, which at Cd is more pronounced than at Hg; this is also shown by the larger width of the cross section resonance. The fact that the spin-orbit interaction seems to be stronger in Cd than in Hg is surprising insofar as Cd is the lighter atom. But this can be understood taking into account that the effective strength of the spin-orbit coupling is not only influenced by Z, but also by interference of states in the autoionizing configuration interaction.

4. Determination of Matrix Elements and Phase-Shift Difference of the Continuum Wavefunctions from the Experimental Results

The experimental quantities σ, β, A and ξ presented in Chap. 3 are functions of two energy-dependent radial dipole matrix elements $R_{1/2}$ and $R_{3/2}$ describing the transition of a bound s-electron into a $\varepsilon p_{1/2}$ or $\varepsilon p_{3/2}$ continuum state, respectively, and of one phase-shift difference $\delta_{1/2}-\delta_{3/2}$ between the two corresponding wave functions of the continuum states. The connection between these two sets of parameters is given by the following equations [9, 18]

$$\sigma=\tfrac{4}{3}\pi^2\,\alpha\,a_0^2\,\omega(R_{1/2}^2+2R_{3/2}^2) \tag{1}$$

$$\beta=\frac{2R_{3/2}^2+4R_{1/2}\cdot R_{3/2}\cdot\cos(\delta_{1/2}-\delta_{3/2})}{R_{1/2}^2+2R_{3/2}^2} \tag{2}$$

$$A=\frac{5R_{3/2}^2-R_{1/2}^2-4R_{1/2}\cdot R_{3/2}\cdot\cos(\delta_{1/2}-\delta_{3/2})}{3(R_{1/2}^2+2R_{3/2}^2)} \tag{3}$$

$$\xi=-\frac{3R_{1/2}\cdot R_{3/2}\cdot\sin(\delta_{1/2}-\delta_{3/2})}{2(R_{1/2}^2+2R_{3/2}^2)} \tag{4}$$

Equations (1) to (4) are the exact formulae for the dissociation channels (photoelectron far away from the remaining ion, i.e. jj-coupling) independent upon which type of coupling [46, 47] describes the autoionizing states best.

For a discussion of these equations, Table 1 shows some special cases indicating the "dynamical relations" between the experimental quantities. The first two lines represent the case of a Cooper minimum, where the two matrix elements go through zero at slightly different energies. Therefore A and β are given by the corresponding value of the non-vanishing channel, whereas ξ as an interference effect vanishes. The third line corresponds to the case of vanishing spin-orbit interaction characterized by

Table 1.

	β	A	ξ
$R_{1/2}=0$	1	5/6	0
$R_{3/2}=0$	0	−1/3	0
$R_{1/2}=R_{3/2}$ $(\delta_{1/2}-\delta_{3/2}=0)$	2	0	0

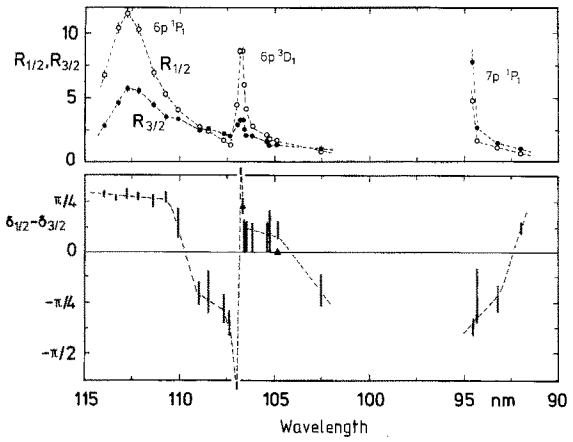

Fig. 6. Upper part: radial matrix elements $R_{1/2}$ (open circles) and $R_{3/2}$ (closed circles). Lower part: phase-shift difference $\delta_{1/2}-\delta_{3/2}$ determined from experimental data of σ [42, 43], β ([15, 16] error bars, [14] triangles), A and ξ. The dashed curves are tentative to guide the eye

only one electronic transition $ns \rightarrow \varepsilon p$ which is treated correctly by non-relativistic theories.

Figure 6 shows the result of the calculations. The dashed curves are tentative curves through the experimental data (error bars) whose number and distances are determined by the β-results. The resonance structure of both matrix elements (upper part) indicates that in all three resonances both partial continua are involved in the interaction between discrete autoionizing and continuum states; however, the coupling strength varies. In the first two resonances the $j=1/2$ channel dominates; in the third resonance the $j=3/2$ channel dominates.

This shows that in the singulet resonances autoionizing states and continua have the same angular momentum j of the photoelectron, i.e. the $6p_{1/2}$ autoionizing state (1. resonance) interacts mainly with the $j=1/2$ continuum, the $7p_{3/2}$ (3. resonance) decays mainly into the $j=3/2$ continuum. In the triplet resonance, however, a spin flip takes place, as was already pointed out in Chap. 3 (Fig. 2) with the consequence that the j value of the autoionizing electron ($j=3/2$) changes to $j=1/2$ of the photoelectrons during the process of autoionization.

The experimental results shown in Fig. 4 in connection with (2) and (3) also allow determination of the phase-shift difference between the $\varepsilon p_{1/2}$ and $\varepsilon p_{3/2}$ continuum wavefunction. The wavelength dependence of this phase-shift difference is also responsible for the resonance behavior, especially in the second (triplet) autoionization resonance. The "experimentally" obtained phase-shift differences are plotted in the lower part of Fig. 6 as error bars (using the β data of [15, 16]) and as triangles (using β data from [14]). Going through the triplet resonance the phase-shift difference changes sign and jumps by π. In the singulet resonances, however, there are no drastic changes as far as data are available.

In Fano's theory of autoionizing resonances [38, 39] the phase shift of the continuum wave function is a sum of the undisturbed phase shift and a contribution Δ due to configuration interaction between the undisturbed continuum state and the discrete autoionizing state. According to [38] Δ varies swiftly by π across the resonance in an energy intervall given by the halfwidth Γ of the resonance. Since the undisturbed phase shift is a slowly varying function of energy, this variation of Δ can also be observed in the total phase shift, as is shown in Fig. 6.

The results show that the spin-orbit interaction which can be regarded to be negligible in direct ionization becomes so strong in the region of autoionization resonances that it almost completely determines the amplitudes and phases of the continuum wave functions.

The absolute sign of the phase difference is directly given by the additional measurement of ξ because of the sine in (4). In fact only the sign of the ξ values measured was needed for the determination of the phase difference. Its absolute value may have been subject to a slight depolarization due to the high electron - Hg scattering cross section [50] at very small electron energies.

5. Conclusions

This paper has shown that spin-polarization results of photoelectrons complement the data of the total cross section and its angular distribution in order to get a complete quantummechanical description of the photoionization process studied. By measuring only three quantities (for s-subshell photoionization) and their energy dependence even such complex structures as autoionization resonances with strongly interacting channels can be understood quantitatively. For the first three autoionization resonances in Hg $6s^2$-photoionization the two matrix elements and one phase-shift difference could be determined. They permit study of the autoionization process in detail. Evidence was found for strong channel interaction between the open and closed channels. The j value of the excited autoionizing electrons could be correlated to the j value of the ejected photoelectrons providing evidence for spin-flip transitions in the triplet resonance. The matrix elements and their ratio vary strongly across the resonances, indicating the strong influence of spin-

orbit interaction on the continuum states in the region of resonances. A change of the relative phase by π across a resonance predicted by Fano has been verified experimentally for the triplet resonance.

We would like to express our gratitude to Professors W. Paul, G. Nöldeke and J. Kessler for their continued interest and encouragement. We thank Dr. D. Husmann, Dr. J. Hormes and B. Osterheld for their assistance in performing the experiment in Bonn. We are grateful to Dr. N.A. Cherepkov for helpful discussions and acknowledge support by the DFG and BMFT.

References

1. Kessler, J.: Polarized Electrons. Berlin, Heidelberg, New York: Springer-Verlag 1976
2. Heinzmann, U.: Appl. Opt. **19**, 4087 (1980)
3. Fano, U.: Phys. Rev. **178**, 131 (1969) and **184**, 250 (1969)
4. Heinzmann, U., Kessler, J., Lorenz, J.: Z. Phys. **240**, 42 (1970)
5. Fano, U.: Commun. At. Mol. Phys. **2**, 30 (1970)
6. Cherepkov, N.A.: J. Phys. B **13**, L 689 (1980)
7. Cherepkov, N.A.: Phys. Lett. **40** A, 119 (1972)
8. Cherepkov, N.A.: Sov. Phys. JETP **38**, 463 (1974)
9. Lee, C.M.: Phys. Rev. A **10**, 1598 (1974)
10. Schönhense, G.: Phys. Rev. Lett. **44**, 640 (1980)
11. Starace, A.F.: Appl. Opt. **19**, 4051 (1980)
12. Amusia, M.Ya., Cherepkov, N.A.: Case Stud. At. Phys. **5**, 47 (1975)
13. Cooper, J., Zare, R.N.: J. Chem. Phys. **48**, 942 (1968)
14. Niehaus, A., Ruf, M.W.: Z. Phys. **252**, 84 (1972)
15. Brehm, B., Höfler, K.: Phys. Lett. **68** A, 437 (1978)
16. Höfler, K.: PhD-Thesis, Universität Hannover (1979)
17. Johnson, W.R., Cheng, K.T., Huang, K.N., Le Dourneuf, M.: Phys. Rev. A **22**, 989 (1980)
18. Cherepkov, N.A.: J. Phys. B **13**, L 181 (1980)
19. Kabachnik, N.M., Sazhina, I.P.: J. Phys. B **9**, 1681 (1976)
20. Kunz, C.: Synchrotron Radiation, Techniques and Applications. Berlin, Heidelberg, New York: Springer-Verlag 1979
21. Schwinger, J.: Phys. Rev. **75**, 1912 (1949)
22. Sokolov, A.A., Ternov, I.M.: Sov. Phys. JETP **4**, 396 (1957)
23. Westfold, K.C.: Astrophys. J. **130**, 241 (1959)
24. Joos, P.: Phys. Rev. Lett. **4**, 558 (1960)
25. Codling, C., Madden, R.P.: J. Appl. Phys. **36**, 380 (1965)
26. Heinzmann, U.: J. Phys. B **13**, 4353 and 4367 (1980)
27. Schäfers, F.: PhD-Thesis, Universität Münster (1981)
28. Schönhense, G.: PhD-Thesis, Universität Münster (1981)
29. Schönhense, G., Schäfers, F., Heinzmann, U., Kessler, J.: Z. Phys. A – Atoms and Nuclei **304**, 31 (1982)
30. Osterheld, B., Schäfers, F., Heinzmann, U.: (to be published)
31. Heinzmann, U.: J. Phys. B **11**, 399 (1978)
32. Cherepkov, N.A.: Phys. Lett. **66** A, 204 (1978)
33. Johnson, W.R., Cheng, K.T.: Phys. Rev. Lett. **40**, 1167 (1978)
34. Ong, W., Manson, S.T.: Phys. Rev. A **19**, 688 (1979)
35. Cheng, K.T., Huang, K.N., Johnson, W.R.: J. Phys. B **13**, L 45 (1980)
36. Samson, J.A.R., Gardner, J.L.: Phys. Rev. Lett. **33**, 671 (1974)
37. Dehmer, J.L., Dill, D.: Phys. Rev. Lett. **37**, 1049 (1976)
38. Fano, U.: Phys. Rev. **124**, 1866 (1961)
39. Fano, U., Cooper, J.: Phys. Rev. A **137**, 1364 (1965)
40. Codling, K., West, J.B., Parr, A.C., Dehmer, J.L., Stockbauer, R.L.: J. Phys. B **13**, L 693 (1980)
41. Beutler, H.: Z. Phys. **86**, 710 (1933)
42. Brehm, B.: Z. Naturforsch. **21a**, 196 (1966)
43. Berkowitz, J.: Photoabsorption, Photoionization and Photoelectron Spectroscopy. New York: Academic Press 1979
44. Garton, W.R.S., Connerade, J.P.: Astrophys. J. **155**, 667 (1969)
45. Mansfield, M.W.D.: Astrophys. J. **180**, 1011 (1973)
46. Martin, W.C., Sugar, J., Tech, J.L.: Phys. Rev. A **6**, 2022 (1972)
47. Martin, W.C., Sugar, J., Tech, J.L.: J. Opt. Soc. Am. **62**, 1488 (1972)
48. Dill, D.: Phys. Rev. A **7**, 1976 (1973)
49. Marr, G.V., Austin, J.M.: Proc. R. Soc. A **310**, 137 (1969)
50. Jost, K., Ohnemus, B.: Phys. Rev. A **19**, 641 (1979)

F. Schäfers
G. Schönhense
U. Heinzmann
Fritz-Haber-Institut der
Max-Planck-Gesellschaft
Faradayweg 4-6
D-1000 Berlin 33
Germany